Pyrrhotite nano-inclusions in apatite from Les Guilleries lamprophyres (NE Iberian Peninsula)

Marina Martínez*,[1] and Mercè Corbella[1]

[1]Dpt. de Geologia, Universitat Autònoma de Barcelona, 08193 Cerdanyola del Vallès (Spain)

Universitat Autònoma de Barcelona

GOLDSCHMIDT LYON 2023

1. INTRODUCTION

- Les Guilleries lamprophyre dykes (LD) (spessartites) represent the **last pulses** of the **least modified magmas** at the end of Variscan magmatism prior to Triassic extension.
- **Apatite** is present in accessory proportions but is ubiquitous in the Les Guilleries LD.
- Apatite can form by a variety of processes, from **primary** igneous crystallization to **secondary** alteration products, and its examination, such as grain sizes, textures, and composition provide useful information about **petrogenetic processes**.

2. GEOLOGIC SETTING

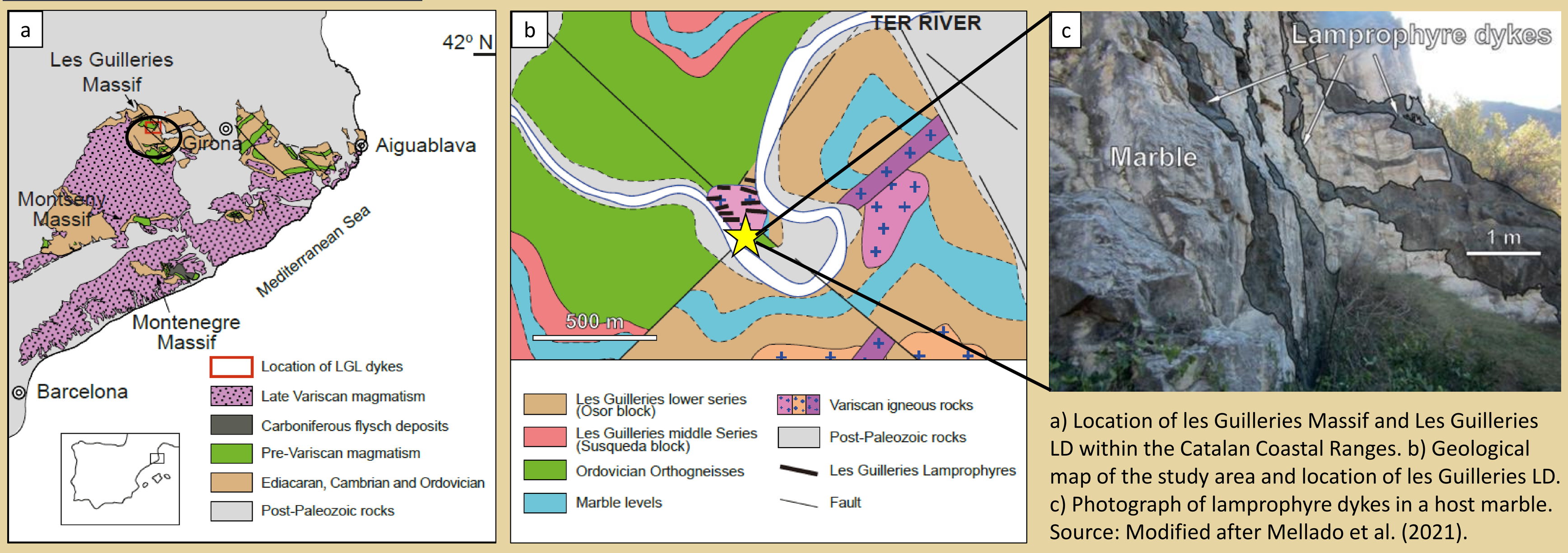

a) Location of les Guilleries Massif and Les Guilleries LD within the Catalan Coastal Ranges. b) Geological map of the study area and location of les Guilleries LD. c) Photograph of lamprophyre dykes in a host marble. Source: Modified after Mellado et al. (2021).

3. ANALYTICAL TECHNIQUES

We have examined two polished thin sections of the lamprophyre dykes emplaced in marble (Fig. 1), numbered GUI-40 and GUI-41, using:

- Optical Light Microscopy (OLM) for general petrography.
- Scanning Electron Microscopy (SEM) for BSE imaging and EDS X-ray analysis of interest sites and apatite grains.
- Electron probe micro-analysis (EPMA) for chemical analyses of apatite grains.
- Transmission electron microscopy (TEM) for BF TEM and DF STEM imaging, SAED patterns, and HR TEM for examination of apatite texture and composition at (sub)micron scales.

4. RESULTS AND DISCUSSION

GUI-40 (least altered)

General petrography of GUI-40

Plagioclase and amphibole, plus chlorite, pyrite, titanite, apatite, allanite, and phlogopite.

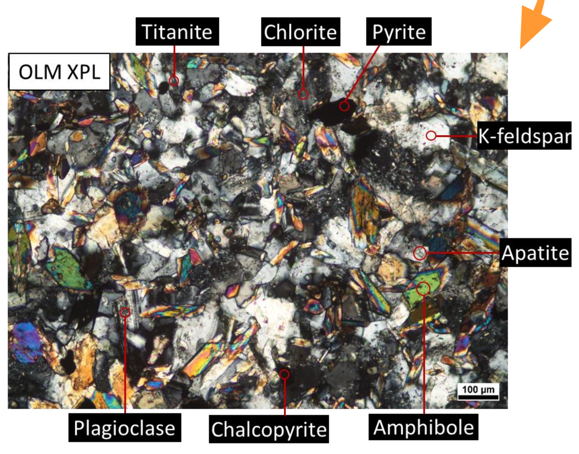

BSE image of a representative region in GUI-40 (a) along with corresponding X-ray compositional RGB (Red-Green-Blue) maps (b-f).

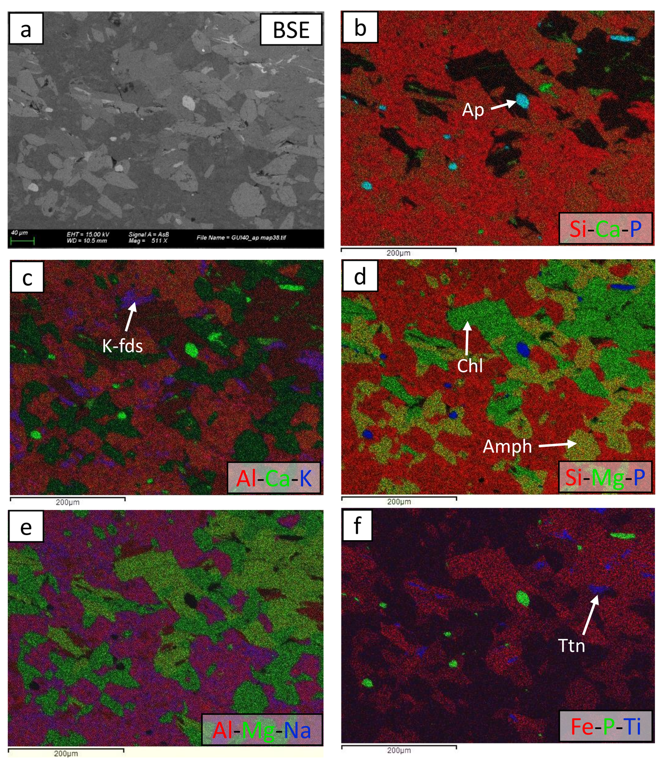

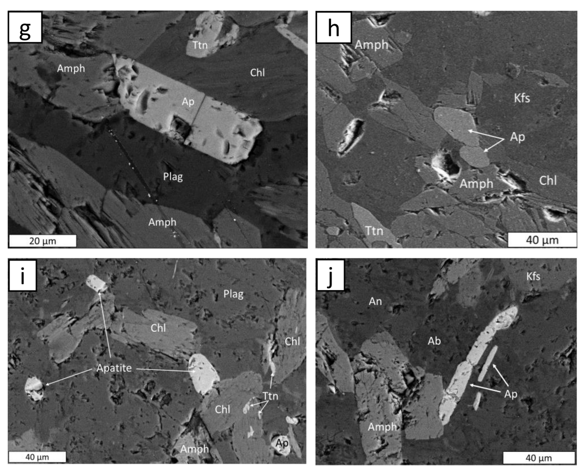

BSE images of apatite grains. Mostly euhedral (g) and subhedral (i-j), up to 50 µm in size, and randomly oriented.

Legend: **Ap** = apatite; **Amph** = amphibole, **Kfs** = K-feldspar; **An** = anorthite; **Ab** = albite; **Plag** = plagioclase; **Chl** = chlorite; **Ttn** = titanite.

GUI-41 (more altered)

General petrography of GUI-41

Altered amphiboles (~300 µm sized) and plagioclase, plus chlorite and calcite (0.5 mm sized). Albite dominates the groundmass. Other phases include titanite, ilmenite, pyrite, chromite, smaller amphiboles, apatite, allanite, epidote, and quartz.

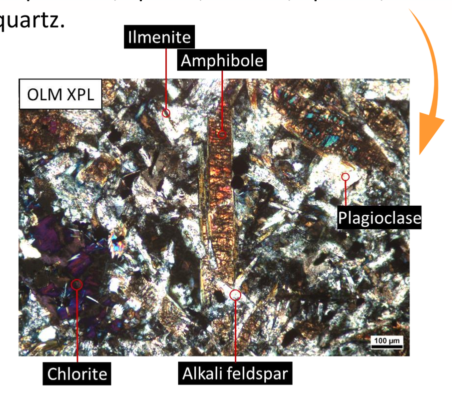

BSE image of a representative region in GUI-41 (a) along with corresponding X-ray compositional RGB (Red-Green-Blue) maps (b-g). Apatite grains shown in (b) as cyan.

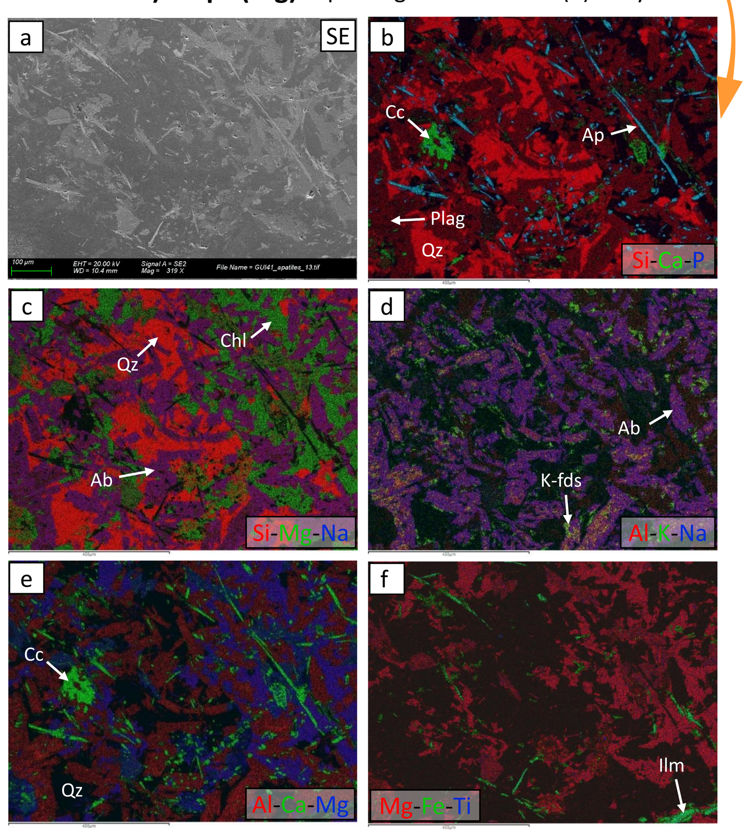

BSE images of apatite grains

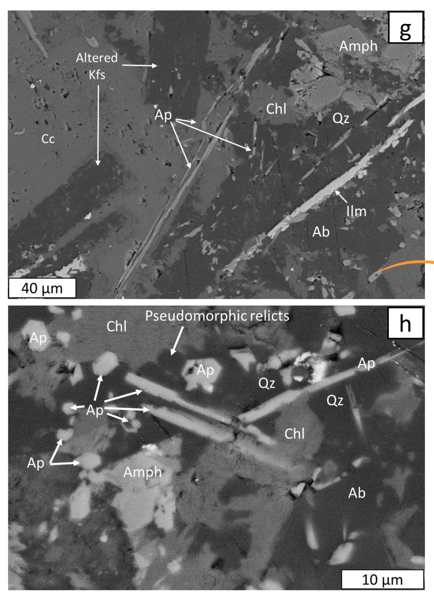

Apatite grains (g,h):

- Range from a few-to-ten µm in width and up to 150 µm in length (**highly acicular**).
- Randomly oriented, heterogeneously distributed, and appear to cut all pre-existing phases, including chlorite and calcite.

Abbreviations: **Ap** = apatite; **Amph** = amphibole; **Plag** = Ca,Na-plagioclase; **Ab** = albite; **K-fds** = K-feldspar; **Chl** = chlorite; **Ilm** = ilmenite; **Qz** = quartz; **Cc** = calcite.

TEM observations (Apatite in GUI-40)

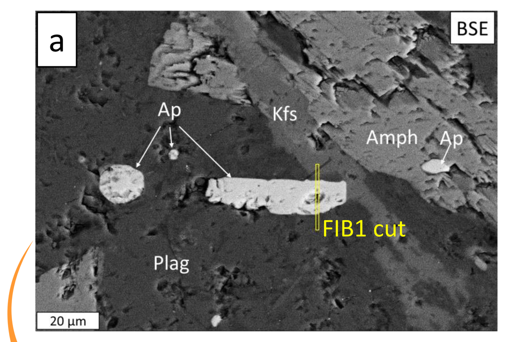

a) BSE image showing the location of the FIB cut. b) HAADF mosaic of the FIB section. Apatite is oriented down the *c* axis ([001] zone axis) and associated with Ab and Kfs.

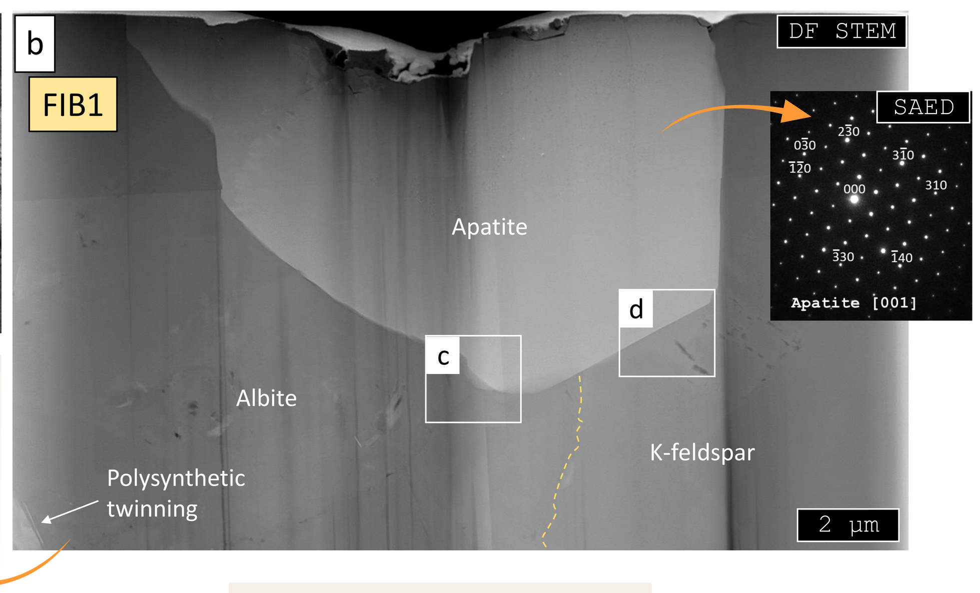

Two types of apatite-feldspar interface (FIB1)

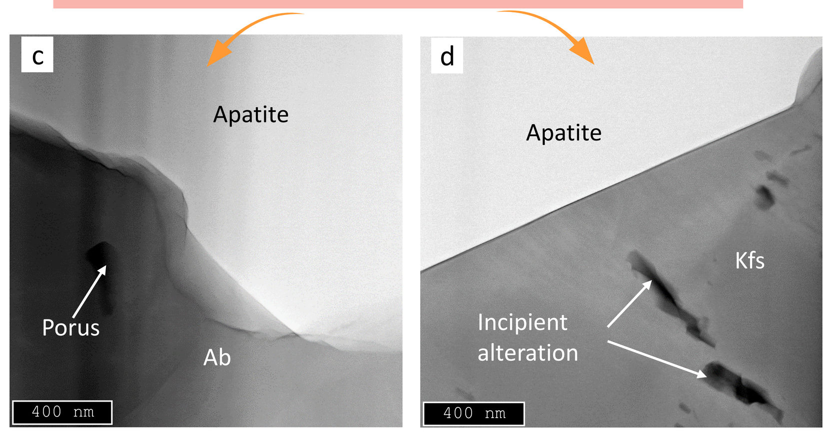

Irregular apatite-albite interface - **Dissolution** (alteration).

Straight and clean apatite-K-feldspar interface. Growth under **equilibrium conditions**.

Inclusions follow the crystallographic orientation of apatite

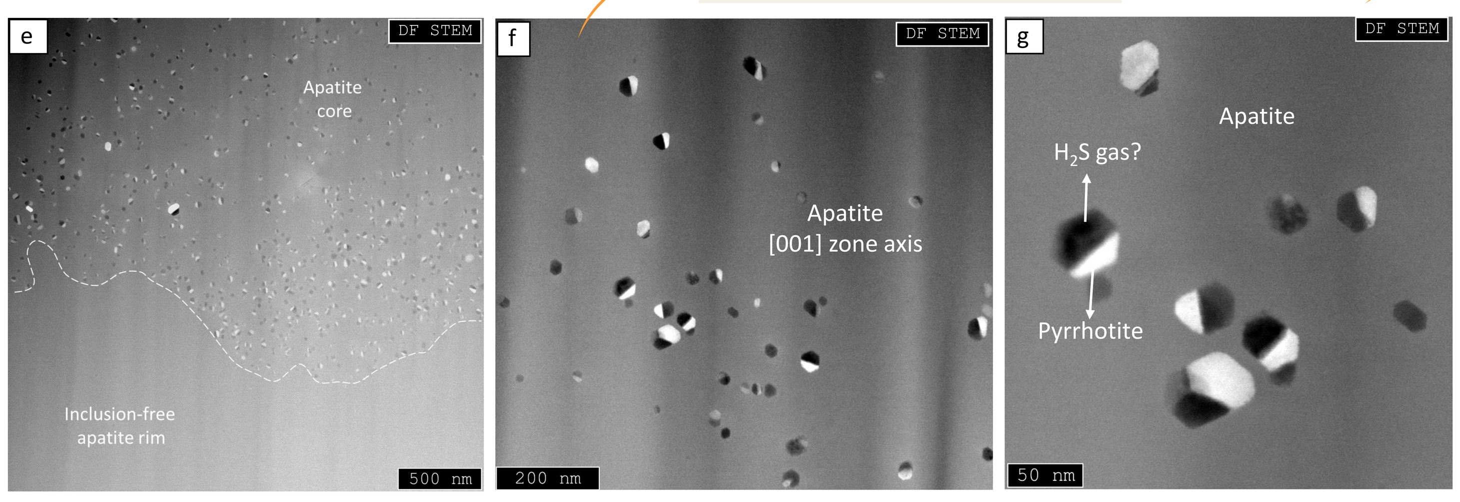

Nano-inclusions within host apatite

- Inclusions only at the **apatite core** (e,l).
- Inclusions are abundant and **similarly oriented** (f,g,m), following the **negative crystal** of apatite.
- Inclusions consist of **pyrrhotite** (h), **pyrrhotite and void** (i), and/or **void space** (j).

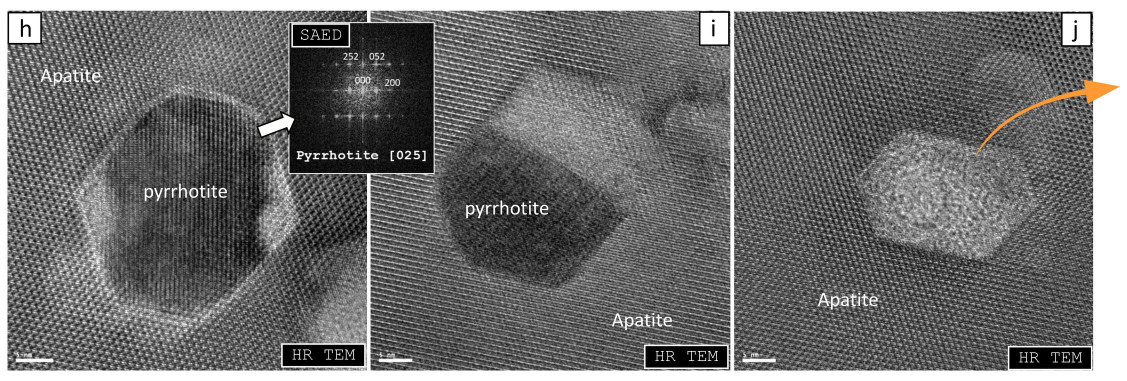

High-resolution TEM image of the low-Z phase = voids

DF STEM line profile of a bimodal inclusion showing the drop of elements at the low-Z phase and the peaks in S and Fe on the high-Z phase.

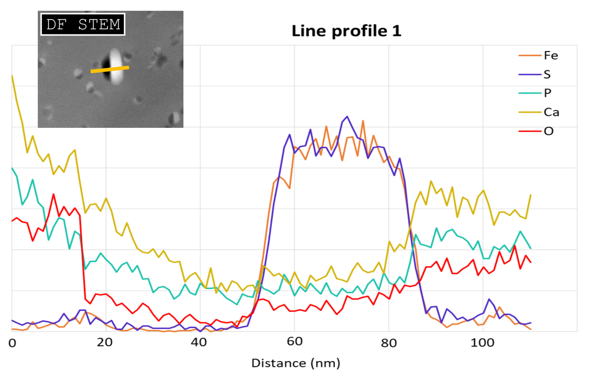

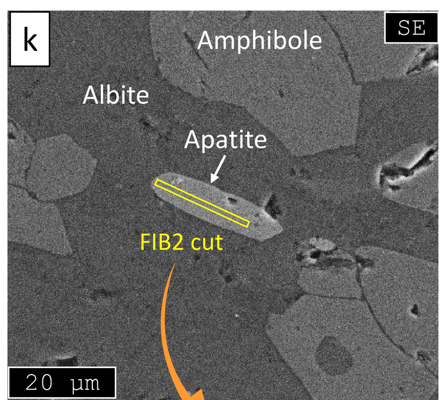

k) SE image showing the location of the FIB cut. **l)** SEM in-lens image of the FIB section during FIB preparation. Apatite is oriented subparallel to the *c* axis.

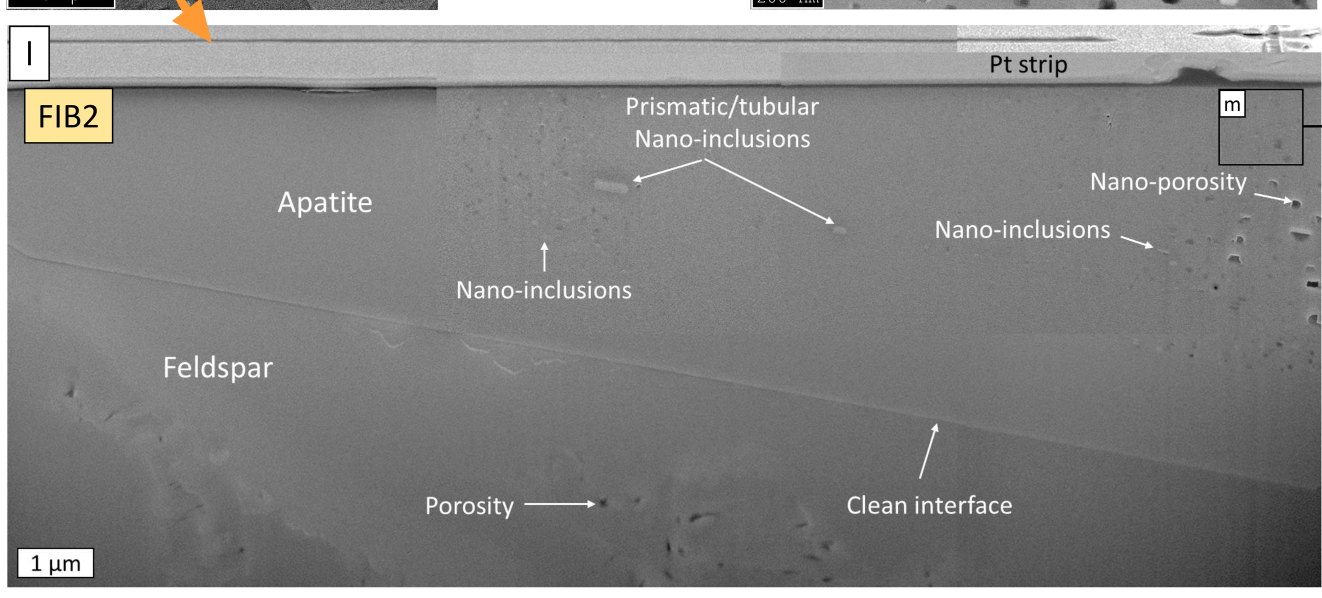

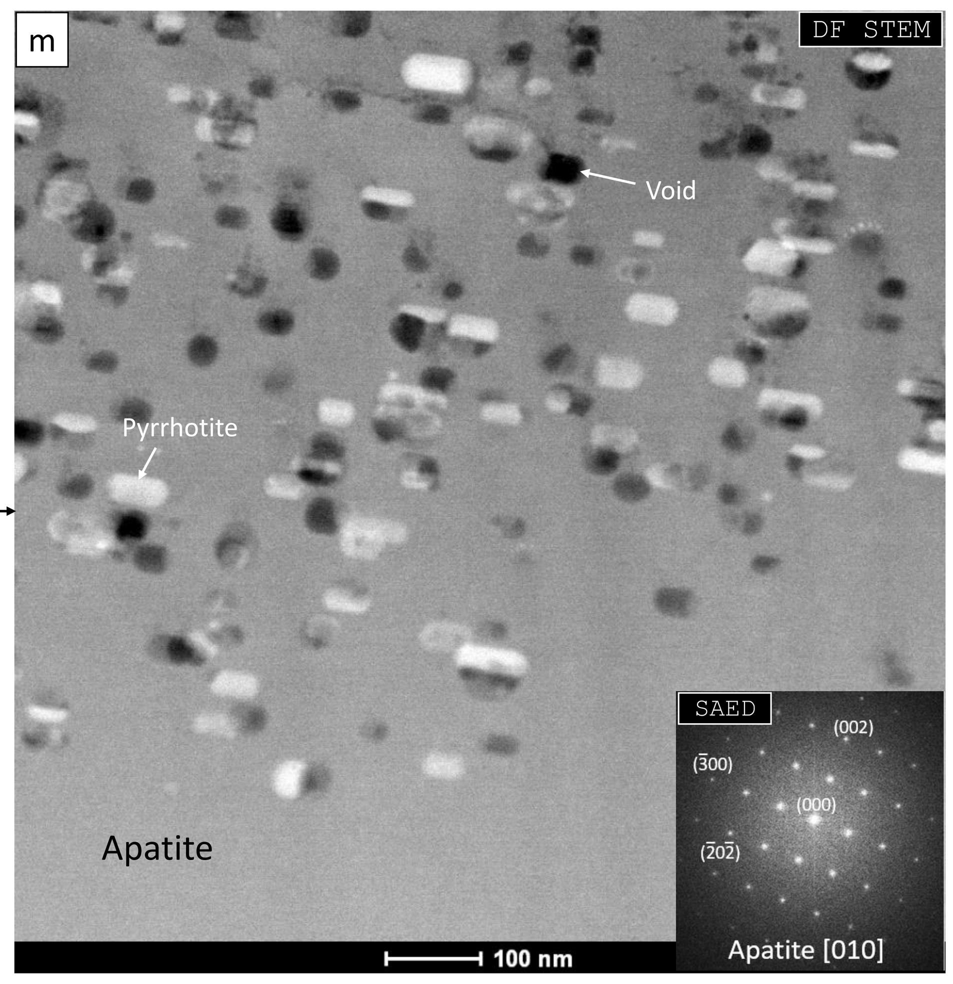

Apatite compositions in GUI-40 and GUI-41 (EPMA)

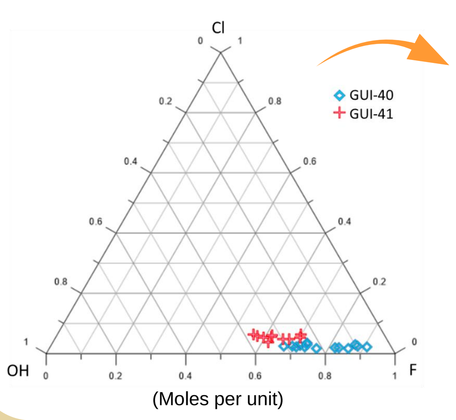

Ternary diagram for Cl-F-OH

- Primary apatites (GUI-40) are F-richer (and Cl-poorer) than secondary apatites (GUI-41).
- **Hydroxyl content is higher in secondary apatites**
- Little to no overlap between the two datasets.

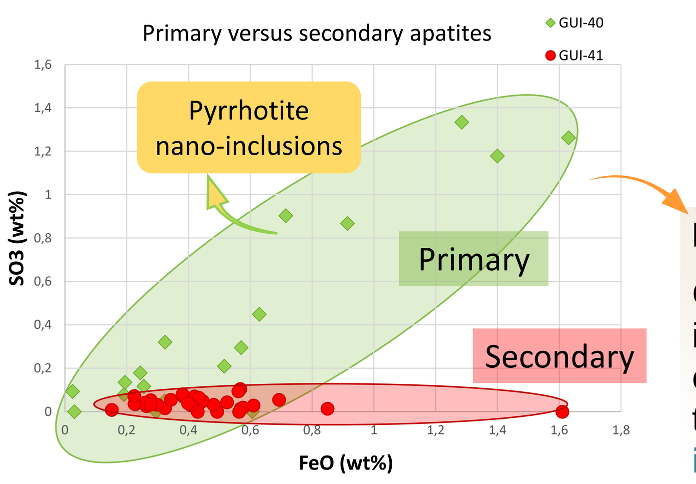

Individual EMPA analysis of apatite grains in GUI-40 and GUI-41

FeO versus SO_3 (wt%) plot

GUI-40 apatite: much larger variability in S and Fe contents in GUI-40 apatites compared to GUI-41 apatites. Attributed to the presence of **pyrrhotite inclusions** observed by TEM.

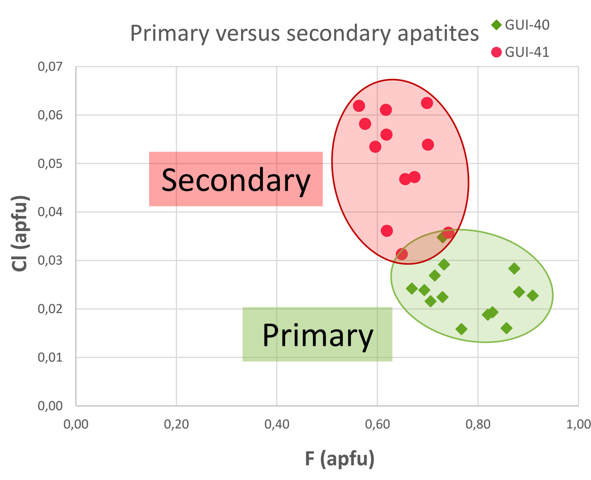

F versus Cl (apfu) plot

Secondary apatites contain slightly **more Cl** than primary apatites, although the Cl content is low in all of them.

5. CONCLUSIONS

- Apatite grains from GUI-40 are **primary**, formed by **igneous crystallization** from the parental lamprophyre magma, whereas apatite grains from GUI-41 are **secondary** products of **hydrothermal alteration**.
- The **parental magma contained some Fe and S**. Sulfur was not incorporated into the apatite structure to form ellestadite domains (as seen in Ferraris et al., 2005) due to the presence of Fe, because Fe is incompatible in apatite.
- TEM work reveals **nano-inclusions of pyrrhotite and void space within host apatite**, following the **negative crystal** of apatite. The parental magma experienced **melt immiscibility** and apatite trapped droplets of a sulfide melt.
- From this study, we conclude that lamprophyres formed under **reducing conditions**.
- This work demonstrates that (sub)micrometer studies of apatite using **TEM** can give valuable insights into parental magmas and processes that are overlooked at the SEM scales (i.e., Martínez et al., 2023a,b).

6. ACKNOWLEDGMENTS

This work was financially supported by the *Ministerio de Ciencia e Innovación* project PID2019-109018RB-I00, awarded to Mercè Corbella. Additional support came through project 2022-SGR-00308 (Consolidate Research Group MAGH) from the Catalan Government. The first author, Marina Martínez, is funded by a Margarita Salas contract with the Spanish Government. Scanning Electron Microscopy was performed at the *Servei de Microscopia* of UAB and EPMA were performed at the *Centres Científics i Tecnològics* (CCIT) of UB. We acknowledge Libertad Solé from the *Institut de Microelectrònica de Barcelona* (IMB-CNM) and Trifon Trifonov from the *Centre de Recerca en Ciència i Enginyeria Multiescala de Barcelona* for their assistance with the SEM-FIB sample preparation. Finally, we thank Belén Ballesteros and Bernat Mundet from *Institut Català de Nanociència i Nanotecnologia* (ICN2) for their assistance with the TEM.

7. REFERENCES

Ferraris, C., White, T. J., Plévert, J., and Wegner, R. (2005) Nanometric modulation in apatite. *Physics and chemistry of minerals* 32, 485-492.

Martínez, M., Shearer, C.K., and Brearley, A.J. (2023a) Nanostructural domains in martian apatites that record primary subsolidus exsolution of halogens: Insights into nakhlite petrogenesis. *American Mineralogist*. Preprint. 10.2138/am-2022-8794.

Martínez, M., Shearer, C. K., and Brearley, A. J. (2023b) Ferro-chloro-winchite in Northwest Africa (NWA) 998 apatite-hosted melt inclusion: New insights into the nakhlite parent melt. *Geochimica et Cosmochimica Acta* 344, 122-133.

Mellado, E., Corbella i Cordomí, M., Navarro Ciurana, D., and Kylander, A. (2021). The enriched Variscan lithosphere of NE Iberia: data from postcollisional Permian calc-alkaline lamprophyre dykes of Les Guilleries. *Geologica Acta* 19, 1-23.

*Corresponding author: Marina.Martinez@uab.cat